Actomyosin Kinetics and in Vitro Motility of Wild-Type *Drosophila* Actin and the Effects of Two Mutations in the *Act88F* Gene

M. Anson,* D. R. Drummond,‡¶ M. A. Geeves,§ E. S. Hennessey,‡ M. D. Ritchie,§ and J. C. Sparrow‡

*National Institute for Medical Research, Mill Hill, London NW7 1AA, United Kingdom; ‡Department of Biology, University of York, York YO1 5DD, United Kingdom; and §Department of Biochemistry, University of Bristol, Bristol BS8 1TD, United Kingdom; and Max Planck Institut für Moleculäre Physiologie, 44026 Dortmund, Germany; ¶School of Biological Sciences, University of Manchester, Manchester M13 9PT, United Kingdom

ABSTRACT Two missense mutations of the flight muscle-specific actin gene of *Drosophila melanogaster, Act88F,* assemble into normally structured myofibrils but affect the flight ability of flies and the mechanical kinetics of isolated muscle fibers. We describe the isolation of actin from different homozygous *Act88F* strains, including wild-type, an *Act88F* null mutant (*KM88*), and two *Act88F* single point mutations (*E316K* and *G368E*), their biochemical interactions with rabbit myosin subfragment 1 (S1), and behavior with rabbit myosin and heavy meromyosin in in vitro motility assays. The rabbit and wild-type *Drosophila* actins have different association rate constants with S1 (2.64 and 1.77 μM^{-1} s^{-1}, respectively) and in vitro motilities (2.51, 1.60 μm s^{-1}) clearly demonstrating an isoform-specific difference. The *G368E* mutation shows a reduced affinity for rabbit S1 compared with the wild type (increasing from 0.11 to 0.17 μM) and a reduced velocity in vitro (reduced by 19%). The *E316K* mutant actin has no change in affinity for myosin S1 or in vitro motility with heavy meromyosin but does have a reduced in vitro motility (15%) with myosin. These results are discussed with respect to the recently published atomic models for the actomyosin structure and our findings that *G368E* fibers show a reduced rate constant for delayed tension development and increased fiber stiffness. We interpret these results as possibly caused either by effects on A1 myosin light chain binding or conformational changes within the subdomain 1 of actin, which contains the myosin binding site. *E316K* is discussed with respect to its likely position within the tropomyosin binding site of actin.

INTRODUCTION

The *Act88F* actin gene of *Drosophila melanogaster* is invaluable for studying the relationship between the amino acid sequence and various functions of actin as it is expressed only in the indirect flight muscles (IFMs) (Fyrberg et al., 1983) and is the sole actin expressed in these muscles (Ball et al., 1987). *Act88F* gene mutations have been selected by the impaired or flightless phenotypes of mutant flies (Mogami and Hotta, 1981; Hiromi and Hotta, 1985; Hiromi et al., 1986; Sparrow et al., 1991); flies with an *Act88F* null mutation are flightless but viable (Hiromi and Hotta, 1985). Furthermore, P-element transformation can be used to transform flies carrying a null mutation with copies of the *Act88F* gene mutated in vitro to study the effects on the structure and function of muscle (Hiromi et al., 1986; Reedy et al., 1989; Drummond et al., 1990, 1991a; Sakai et al., 1990, 1991).

Two *Act88F* mutations that cause single amino acid replacements, *G368E* and *E316K,* when introduced into the germline of flies as the only functional gene copies, produce IFMs containing normal amounts of actin (Drummond et al., 1990). The IFMs have wild-type myofibrillar ultrastructure. Whereas *G368E* flies fly poorly with a wingbeat frequency reduced by approximately 30%, *E316K* flies do not fly. Mechanical experiments on skinned IFM fibers from each mutant produced tension transients in which the principal changes were in the rate constants of the delayed tension rise following a quick stretch in an active contraction. The rate constant was reduced by approximately 30% for *G386E* and increased by a similar amount for *E316K*. There was also an increased fiber stiffness in the *G368E* fibers measured under rigor conditions, or by the in-phase stiffness when a fast step length increase was applied to the fibers in activating conditions (Drummond et al., 1990).

Interpretation of these mechanical results is limited by our current knowledge of the roles of individual amino acids within the actin molecule and actin's interactions with myosin, which lead to tension generation. To investigate the effects of the mutants on actin interactions with myosin, it is necessary to examine the effects of these point mutations on the dynamic properties of actomyosin in vitro and to correlate these with measurements on the muscle fibers. Based on the atomic structures of rabbit actin (Kabsch et al., 1990; Holmes et al., 1990) and myosin subfragment 1 (S1) (Rayment et al., 1993b), models have been constructed of the docking of actin with myosin S1 (Rayment et al., 1993a; Schroeder et al., 1993) from which the interactions in the rigor complex at the near-atomic level may be deduced.

We report here the extraction and characterization of *Drosophila* actin from wild-type, an *Act88F* null strain *(KM88),* and two mutant strains, *G368E* and *E316K*. The interaction of wild-type *Drosophila* actin with rabbit myosin and its proteolytic subfragments, S1 and heavy meromyosin (HMM), is compared with rabbit muscle actin (RSA) by in vitro motility assays and in equilibrium, steady-state, and transient kinetic studies in solution. We have investigated quantitative changes in actomyosin interactions resulting

Received for publication 18 April 1994 and in final form 2 February 1995.

Address reprint requests to Dr. John C. Sparrow, Department of Biology, University of York, York YO1 5DD, UK. Tel.: 011-44-1904-432826; Fax: 011-44-1904-432860; E-mail: jcs1@unix.york.ac.uk.

0006-3495/95/05/1991/13 $2.00

from the *E316K* and *G368E* mutations. Although the *Drosophila* actins preparation contained considerable proportions of non-IFM actin isoforms in addition to the IFM-specific *Act88F* actin and its ubiquitin conjugate, arthrin, significant quantitative differences were detected between the wild-type controls and the mutant actin preparations.

MATERIALS AND METHODS

Actin mutations

Creation of *Drosophila* strains transformed with the *Act88F* gene mutations *E316K* and *G368E* was described in Drummond et al. (1991a). Mutant nomenclature is based on the single letter amino acid code and the codon number; e.g., *E316K* is a change from glutamate to lysine at residue 316.

Protein purification/preparation

Drosophila actin

Wild-type *Drosophila* actin was made from flies of the homozygous ry^{506} strain (ry^{506} is an allele of the *rosy* eye-color gene) and from ry^{506} with the actin null mutant, $Act88F^{KM88}$ (Hiromi and Hotta, 1985), which expresses no Act88F actin in the IFMs. Mutant actins were also prepared from ry^{506} $Act88F^{KM88}$ e^{s} flies with, additionally, two P-element transformed copies of the mutant *Act88F* gene.

Flies were collected and stored at −20°C before processing. Myofibrils were prepared from 100 g of flies as described by Saide et al. (1989) and then stored in York modified glycerol (White, 1983) at −20°C. An acetone powder was prepared from the myofibrils and extracted in a solution (ACEX) containing 10 mM Tris, pH 8.0, 0.5 mM ATP, 0.2 mM $CaCl_2$, 1 mM dithiothreitol (DTT) as described by Bullard (1973) after Pardee and Spudich (1982). The extract was centrifuged at 60,000 *g* for 20 min at 4°C in a Beckman 70.1 Ti rotor to pellet debris. At this stage the *Drosophila* actin preparation still contained other thin filament proteins, which were removed by raising the salt concentrations to 75 mM KCl and 2 mM $MgCl_2$ to induce actin polymerization. The KCl concentration was then increased to 1.06 M. After incubation at 37°C for 30 min (Szilagyi and Chen Lu, 1982), the F-actin was pelleted at 220,000 *g* in the 70.1 Ti rotor for 1 h at 20°C. The actin pellet was rinsed with 75 mM KCl and 2 mM $MgCl_2$ and resuspended in the ACEX buffer, and the actin was stored in aliquots at −80°C.

Rabbit actin

For biochemical experiments, rabbit G-actin and F-actin were made as described by Lehrer and Kerwar (1972). The actin was pyrene labeled (pyr. actin) as described by Criddle et al. (1985). Molar concentrations of actin were determined at 280 nm with an extinction coefficient of $A_{280} = 1.104$ cm^2/mg after correcting for the absorbance of the pyrene label.

Actin for the motility assays

For the in vitro motility experiments the *Drosophila* and rabbit F-actins were labeled with rhodamine-phalloidin. RSA was purified according to Pardee and Spudich (1982), and concentrations were estimated with $(A_{290} - A_{310}) = 0.63$ cm^2/mg. Before use, the F-actin suspensions were incubated on ice in HAB buffer (25 mM HEPES/HCl, pH 7.5, 25 mM KCl, 4 mM $MgCl_2$, 1 mM EGTA, and 2 mM DTT) at 1 μM concentration with 1.5 μM rhodamine-phalloidin (Faulstich et al., 1988) for several hours in light-tight containers. The fluorescently labeled F-actin filaments were typically 1–10 μm long and stable for several days when kept on ice in the dark.

Myosin, S1, and HMM

Myosin was prepared from fast-twitch muscles of the back and hind legs of rabbits by a procedure modified from that of Margossian and Lowey (1982) and then stored at −20°C in 50% (v/v) glycerol where it was stable for several months. The concentration was estimated spectrophotometrically with an extinction coefficient of $A_{280} = 0.53 cm^2/mg$ (Margossian and Lowey, 1982). This myosin was either used directly after dilution in high salt buffer or as the starting material for proteolytic digestion. S1 was prepared by chymotryptic digestion of myosin as described by Weeds and Taylor (1975) and the molar concentrations determined from $A_{280} = 0.77$ cm^2/mg. HMM was prepared by incubation of myosin with α-chymotrypsin according to the method of Margossian and Lowey (1982) with minor modifications. After centrifugation to remove the light meromyosin tails and undigested myosin, the supernatant was used without further purification steps. The HMM was stored on ice and remained stable for several days. Molar concentrations were measured spectroscopically with $A_{280} = 0.60$ cm^2/mg.

The myosin for motility assays was further purified to remove those molecules that bound actin irreversibly. Myosin, 2.4 mg/ml in MAB buffer (as HAB buffer but 600 mM KCl and 5 mM DTT), was reacted on ice with a threefold molar excess of RSA. ATP was added to 10 mM and the mixture spun in a Beckman TLX centrifuge (TLA120.2 rotor at 100,000 rpm for 15 min at 2°C). The supernatant was removed, stored on ice, and used within a few hours.

Reagents

N-methylanthraniloyl derivatives of ATP and ADP (mantATP/ADP), prepared and characterized by the method of Hiratsuka (1983), were a kind gift of Dr. J. F. Eccleston (NIMR, London, UK). Rhodamine-labeled phalloidin was a gift from Prof. H. Faulstich (Max-Planck-Institut für Medizinische Forschung, Heidelberg, Germany) and prepared following the method of Faulstich et al. (1988). All other reagents were of Analar grade and used without further purification.

Kinetic measurements

S1 ATPase

G-actin was polymerized as in the actin preparation method and the F-actin pellet recovered after centrifugation in a Beckman TL100 for 15 min at 15°C and a speed of 100,000 rpm, washed twice in low ionic strength ATPase assay buffer (3.5 mM KCl, 2 mM $MgCl_2$, and 1 mM Tris, pH 8.0), resuspended in this buffer, and then incubated overnight at 4°C. The rabbit S1 was dialyzed against three changes of assay buffer at 4°C overnight. The assays were performed at 20 ± 1°C in a total volume of 15 μl. Each assay contained 1 μM S1, 2 mM ATP, and a variable concentration of actin. The actin concentration in each assay was determined by one-dimensional sodium dodecyl sulfate polyacrylamide gel electrophoresis (SDS-PAGE), Coomassie staining, and densitometry with bovine serum albumin (BSA) protein standards. This method gave quantitation of rabbit actin samples that agreed with the A_{280} readings. The assay was initiated by addition of ATP. After 2-μl aliquots were removed from each assay at regular time intervals, the reaction was quenched into 18 μl of 0.6 M monobasic ammonium phosphate and then stored at 4°C until analyzed. Each assay was performed three times during the same day. ATP and ADP in the samples were separated by high pressure liquid chromatography on an ion exchange column, the peaks were cut from the trace, and their areas were determined by weighing.

Fluorescence titrations and transient kinetics of actin-S1 interactions

Stopped-flow experiments were performed at 20°C with a Hi-Tech Scientific SF-51 stopped-flow spectrophotometer (Ritchie et al., 1993). The transients shown are the average of 3–5 consecutive pushes of the stopped-flow, and concentrations refer to the concentrations of reactants after mixing in the stopped-flow cell.

Fluorescence titrations were carried out on a Perkin-Elmer LS 5B luminescence spectrophotometer, thermostatted at 20°C, with excitation/emission bandwidths of 2.5 nm. Typical working volumes of 600 μl were used.

Motility assay

The actin in vitro motility assays (Kron and Spudich, 1986; Warrick et al., 1993) were performed on an inverted microscope (Zeiss Axiovert 35, Carl Zeiss, Oberkochen, Germany) essentially as detailed by Anson (1992) with the following changes. The rhodamine fluorescence was excited at 436 nm by a high pressure mercury arc lamp (HBO 100W/2) with a Zeiss rhodamine filter set 15. The flow cell had a volume of approximately 40 μl. Myosin was introduced in two 50-μl aliquots at 100 μg/ml from high salt MAB buffer. HMM was used at 30 μg/ml in HAB buffer. Excess myosin or HMM was washed out with HAB containing 0.5 mg/ml BSA, which also served to block vacant protein binding sites on the nitrocellulose surface. A volume of 100 μl of labeled actin (10 nM) was then added in HAB buffer containing BSA. Excess actin was washed out with HAB buffer containing 0.5 mg/ml BSA with 100 μg/ml glucose oxidase, 18 μg/ml catalase, and 3 mg/ml glucose as an oxygen-scavenging, anti-fade combination to reduce the rate of fluorescence photobleaching (Kron et al., 1991). The flow-cell was transferred to the microscope and actin filaments observed in rigor. Movement was initiated by adding 100 μl of HAB containing BSA, the anti-fade enzyme combination, and 2 mM ATP. The microscope stage and objective lens were temperature controlled (Anson, 1992) and flow-cell temperature was measured (±0.2°C) with a thin-film platinum resistance probe. All experiments were performed between 24.7 and 25.5°C.

Modifications to the set-up and procedures for data storage and analysis (Anson, 1992) included a time-date generator (VTG 33, Fora Co., Japan) that superimposed the date and time (to 2 ms) on each image field from the image processor before recording on S-VHS videotape with a Panasonic 7330 VCR (Matsushita Electric Co., Osaka, Japan). Recordings were processed off-line. For machine analysis by the expert vision tracking system (Celtrak, Motion Analysis Corp., Santa Rosa, CA), the CCIR images were converted from PAL to NTSC by a multistandard Panasonic NV-W1 VCR (Matsushita Electric Co.) and recorded on VHS videotape. Tape segments were selected for good quality of recording and freedom from microscope stage movement or focusing. Procedures for the use of this automatic tracking system are discussed by Homsher et al. (1992) and Sellers et al. (1993). The filament centroids were digitized in real time, frame by frame, with the VP 110 video processor and filed on a Sun SPARC IPC computer (Motion Analysis Corp.). The centroids were joined up to form individual filament paths that were displayed graphically on the computer VDU in an interactive mode. This facilitated the editing of individual paths with clearly anomalous tracks, such as jumps or breaks, to leave straight or gently curving paths with a minimum length of several micrometers. Spiraling or rotating filaments were eliminated. The edited path files were processed to extract the mean filament speed and individual standard deviation, and these were then combined to calculate the average filament velocity and its statistical parameters.

RESULTS

Actin purity

As determined by one-dimensional SDS-PAGE (not shown), the IFM actin preparations contained 90% actin and arthrin, an actin-ubiquitin conjugate of *Act88F* actin (Ball et al., 1987). The contaminants were thin filament proteins including tropomyosin, troponins, and troponin-H.

On two-dimensional gels, the actin from wild *Drosophila* migrates as three distinct spots, numbered, from acidic to basic, as I, II, and III (Horovitch et al., 1979). Spots I and II were provisionally identified as type I and II actins from the abdomen, leg, and head (Horovitch et al., 1979). The wild-type actin preparations show one minor and three major spots (Fig. 1). The most basic spots are the mature form of the *Act88F* gene actin (III) and arthrin. The prominent, more acidic spot (II) is incompletely processed actin from the *Act88F* gene (Mahaffey et al., 1985) and the product of the

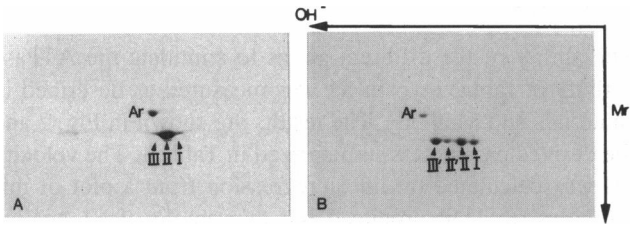

FIGURE 1 2-D electrophoresis of (*a*) *Drosophila* wild-type (wild-type) and (*b*) *E316K* actin preparations. First dimension ampholines (Pharmalyte) pH 5–7 1.6% and pH 3–10 0.4%; second dimension gel acrylamide concentration 12.5%. Ar, arthrin; actin III, mature *Act88F* actin; actin II, unprocessed *Act88F* actin + *Act79B* actin; actin I, cytoplasmic actin. Actin III′ and actin II′ are *Act88F* isoforms encoded by the *E316K* actin gene.

Act79B gene, expressed in other adult muscles (Fyrberg et al., 1983). The minor, more acidic spot (I) is cytoplasmic actin (Horovitch et al., 1979) encoded by the *Act5C* and *Act42A* genes (Fyrberg et al., 1983). This spot is not seen in two-dimensional gels of demembranated myofibrils (Drummond et al., 1990), and in these samples the major actin spot is *Act88F* actin with a smaller, unprocessed fraction at the actin II position. In the two-dimensional gels of the *G368E* preparations (not shown), because of the mutant's charge change (G, glycine, to E, glutamate) the *Act88F* comigrates with the *Act79B* actins at the actin II position and cytoplasmic actins at the I position. The *E316K* actin preparations show five spots (Fig. 1); three spots (arthrin, *Act88F*(III), *Act88F*-(II)) identified above have moved as a result of the charge change (E, glutamate, to K, lysine) and two other spots (*Act79B*(II) and the cytoplasmic actin). The charge change of the *E316K* actin therefore reveals the *Act79B* protein. Thus, a reliable estimate for the isoform purity of the *Act88F* actin was possible only for the *E316K* actin. From densitometer scans of the *E316K* gels, the fractions of the total actin represented by different actins were estimated as: arthrin, 5.9%; *Act88F* spot 2, 24.8%; *Act88F* spot 1, 10.7%; type II, 34.1%; and type I, 24.5%; i.e., 41.4% of the total actin and arthrin present are *Act88F* isoforms and the remainder (58.6%) are types I and II. Because the actin preparation protocols involve repeated cycles of polymerization and depolymerization, we assume that the F-actin filaments contain the actin isoforms in these proportions.

The yields of the actins from wild-type, *E316K*, and *G368E* flies are similar, therefore we believe that the levels of different isoforms in each preparation can be assumed to be approximately the same. Thus, the characterization of the *Drosophila* actins described below must be viewed in the context of the known isoform content of the *E316K* actin and the probable mix of the wild-type and *G368E* actin isoforms. We therefore prepared actin from the *KM88* null mutants in an attempt to characterize these contaminating isoforms. When differences are seen between the wild-type and the *E316K* and *G368E* mutant actins, these must reflect the changes in the 40% of the actin encoded by the *Act88F* gene. The presence of other actin isoforms will cause the effects of any mutation to be underestimated.

S1 ATPase

The ability of the different actins to stimulate the ATPase activity of rabbit myosin S1 was measured as described in Materials and Methods. The results are shown in Fig. 2 and the derived parameters summarized in Table 1. The velocity (v) was calculated by linear regression from a plot of micromoles of ADP produced per micromole of S1 against time. All r values (regression coefficients) were >0.9. Rates of <1 s^{-1} gave low r values as a result of inaccuracy in quantifying the small amounts of ADP produced and were not included in subsequent analysis. From v plotted against v/[actin] (Eadie-Hofstee plot) the V_{max} and K_{app} (actin concentration required for activation of 50% V_{max}) were determined. In the absence of actin, the S1 had an average turnover rate of 0.145 s^{-1} (range 0.03 to 0.341). The values of V_{max} for the S1 ATPase on addition of the different actins were indistinguishable. However, the K_{app} obtained with rabbit actin was significantly lower than the values obtained with any of the *Drosophila* actins. No significant differences were observed between the K_{app} values obtained for the three *Drosophila* actin preparations.

Fluorescence titrations of actin and S1

The fluorescence of mantADP (excitation, 350 nm; emission, 440 nm) is enhanced by a factor of 2.6 on binding to S1, and it binds with a dissociation constant, K_d, of 0.2 μM (Woodward et al., 1991). The affinity of mantADP for acto-S1 is greatly reduced with a K_d equal to 120 μM. Therefore, the addition of actin to a 0.5-μM S1-mantADP complex results in release of the bound nucleotide analogue and a decrease in fluorescence. Fluorescence titration of the S1-mantADP complex with actin, then, affords a rapid and economical means to measure the binding of unlabeled actin to S1. Fig. 3 *a* shows a titration performed with *E316K* actin at low ionic strength conditions in which the S1 concentration greatly

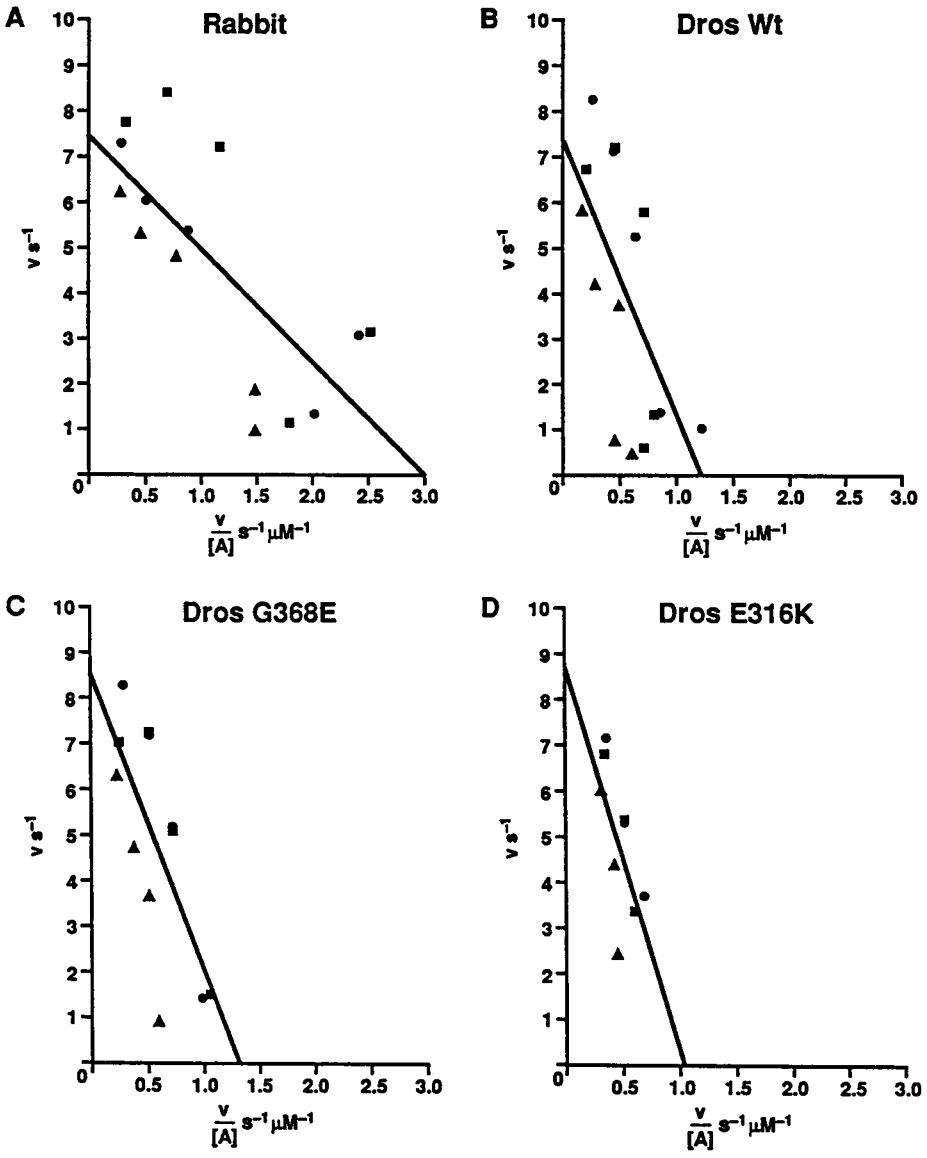

FIGURE 2 Eadie-Hofstee plots for actin activation of rabbit myosin S1 Mg.ATPase activity by rabbit and *Drosophila* actins. Values of V_{max} and K_m are provided in Table 1.

TABLE 1 Kinetic measurements of *Drosophila* wild-type and mutant actin binding to rabbit S1

Measured parameter	Actin			
	RSA	*Drosophila* wild-type	*G368E*	*E316K*
V_{max} (s^{-1})	7.5 ± 2.1*	7.3 ± 1.7	8.5 ± 2.0	8.4 ± 2.3
K_{app} (μM)	2.5 ± 1.1	6.1 ± 2.2	6.5 ± 2.7	8.1 ± 4.7
k_{ATP} (μM^{-1} s^{-1})	2.77	2.8	2.61	
K_{ADP} (μM)	178	152	179	
k_{on} (μM^{-1} s^{-1})	2.64	1.77	1.54	1.99
k_{off} (s^{-1})	0.10	0.11	0.27	0.11
k_{off}/k_{on} (μM)	0.037	0.062	0.175	0.054
K_d (μM)	0.10	0.11	0.17	0.12

Results for V_{max} and K_{app} are given as mean ± SE.

exceeds the expected K_d value of S1 for actin. Stoichiometric binding is observed and allowed the concentration of actin to be determined. Fig. 3 *b* shows a titration with *G368E* at higher ionic strength (0.1 M KCl) at which the S1 concentration used is close to the expected value of K_d, and K_d was determined from analysis of the resulting binding curve. Similar titrations were performed at both high and low ionic strength for actin from rabbit, wild-type, *E316K*, and *G368E* and low salt titrations for actin from *KM88*. The concentrations of the four *Drosophila* actins determined by titration at low salt concentration were in close agreement with those determined from the $A_{280\ nm}$ with the rabbit actin extinction coefficient. Thus, all four actin preparations are capable of making the rigor-type interactions with S1.

The dissociation constants for rabbit, and the three Drosophila actins are shown in Table 1. The value for rabbit actin is in good agreement with previous measurements (Criddle et al., 1985). The affinity of both the wild-type and *E316K* actin for S1 were indistinguishable from that of rabbit actin. However, a significant lowering in affinity of *G368E* actin for S1 was apparent. This could be a result of a reduced rate of association (k_{on}) of the actin and S1, an increased rate of dissociation (k_{off}) of the acto-S1 complex, or a combination of the two.

The rate of association of actin with S1

The rate of association of S1 with each actin species was monitored using 90° light scattering in the stopped-flow fluorimeter. Fig. 4 shows data from an experiment in which 0.5 μM *E316K* actin was reacted with 12.5 μM S1. The data were fitted to a single exponential with a sloping baseline, and the least squares best fit is shown superimposed. The slower component of the scattering is thought to be caused by aggregation, a phenomenon also noticed during steady-state experiments. This aggregation was apparent for all of the *Drosophila* actins but not seen with rabbit actin. The second order rate constant, k_{on}, for the binding of S1 to actin was determined from the linear dependence of the observed rate constant (k_{obs}) on S1 concentration and is shown in Fig. 4 *b* for all actins. These gave values of 2.64 (rabbit), 1.77 (wild-type), 1.99 (*E316K*), 1.54 (*G368E*), and 1.66 (*KM88*)

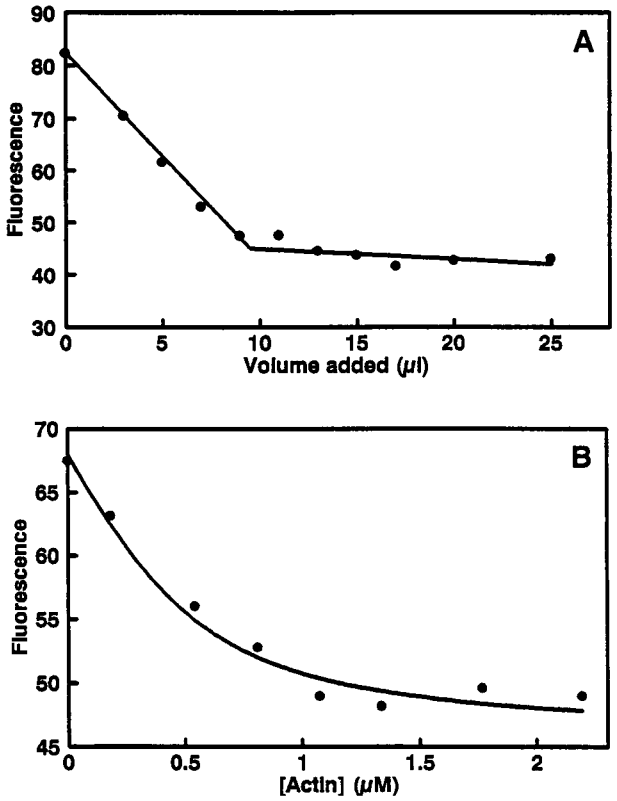

FIGURE 3 Fluorescence titration of S1-mantADP with actin. (*a*) Titration of 600 μl of 0.6 μM mantADP and 0.5 μM S1 with *E316K* actin at low ionic strength. Conditions: 50 mM cacodylate, 5 mM $MgCl_2$, pH 7, 20°C. mantADP fluorescence was excited at 360 nm and emission monitored at 440 nm. (*b*) High salt titration with *G368E* actin; buffer as in *a* but including 0.1 M KCl.

μM^{-1} s^{-1}. Differences between the values for the *Drosophila* actins are within the limits of experimental error but are all significantly lower than that for rabbit actin.

The rate of dissociation of the acto-S1 complex

Fig. 5 shows the displacement of *G368E* actin from 0.5 μM acto-S1 by addition of 14 μM rabbit pyr.actin. The observed exponential decrease in pyrene fluorescence (k_{off}) that occurs as the pyr.actin binds to S1 was followed by a marked linear fall in signal. The linear component of the signal change was apparent for all actins and was attributed to a combination of fluorescence bleaching and aggregation. When the experiment was repeated but with displacing of rabbit pyr.actin by addition of a large excess of unlabeled rabbit actin (possible only for the rabbit actins), a similar exponential rate was observed although with a greatly reduced linear phase. The observed exponential rate constant was independent of the concentration of added pyr.actin for all of the actins. Little difference was observed between the values of k_{off} for rabbit (0.10 s^{-1}), wild-type (0.11 s^{-1}), *KM88* (0.09 s^{-1}), and *E316K* (0.11 s^{-1}) actins. There is, however, a clear increase in the value observed for the *G368E* actin (0.27 s^{-1}), a result compatible with the reduced affinity of this actin for S1 (Table

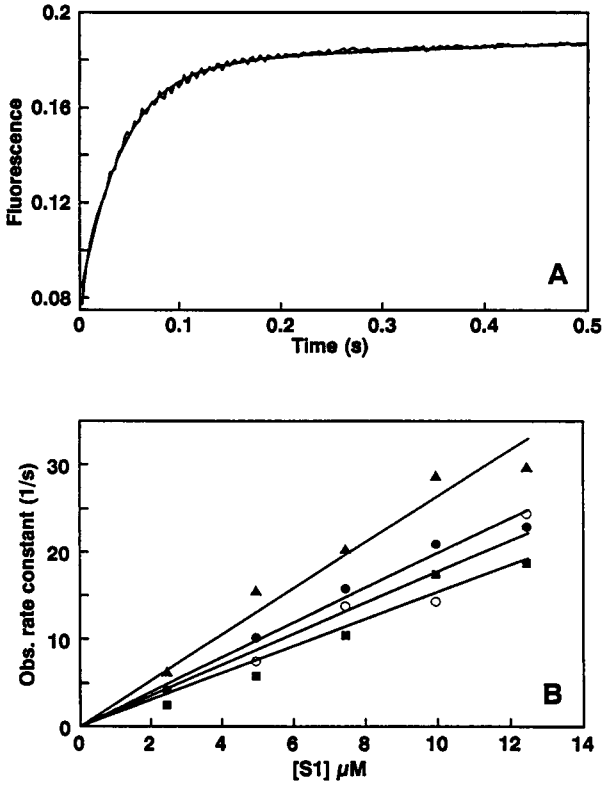

FIGURE 4 The rate of association of S1 with the four actin types. (*a*) The increase in light scattering observed on mixing 0.5 μM *E316K* actin with 12.5 μM S1 in the stopped-flow apparatus. The transient is an average of three successive records and is shown with the best fit single exponential with slope superimposed. k_{obs} = 23.1 s^{-1}. (*b*) Dependence of k_{obs} on S1 concentration. △, rabbit; ○, wild-type; ●, *E316K*; ■, *G368E*. Second order rate constants were obtained from the gradient of the best fit linear regression lines and are shown in Table 1. Conditions are as in Fig. 3 *b*.

1). The ratio k_{off}/k_{on} gives an independent measure of K_d and clearly shows that binding to S1 is similar for RSA, wild-type, *KM88*, and *E316K* but weaker for *G368E* actin. However, for the RSA, wild-type, and *E316K* actins, this gives values that are approximately one-half of those obtained from the titration measurements with a difference between the RSA and the other two, which reflects the decrease in k_{on}. Titrations rarely give a value of K_d that is defined to better than a factor of two in this range. The estimates from the ratio of k_{off}/k_{on} may therefore be more accurate.

The interaction of ATP and ADP with acto-S1

The ATP-induced dissociation of acto-S1 was followed by using light scattering in the stopped-flow fluorimeter. In all cases the observed signal change was well fitted by a single exponential (data not shown). At relatively low ATP concentrations (5–25 μM), the observed rate of dissociation was linearly dependent on ATP concentration, the slope defining the second order rate constant (k_{ATP}) for the binding of ATP to acto-S1. The results showed no significant effects of the different actins on the rate of ATP binding to the complex, which was 2.7 (±0.1) μM^{-1} s^{-1} in all cases. The affinity of

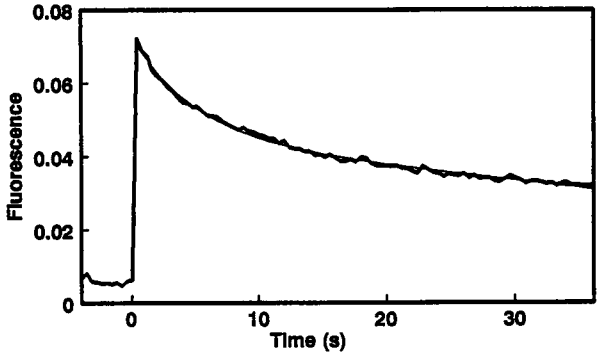

FIGURE 5 The fluorescence change accompanying the displacement of *G368E* actin from the acto-S1 complex by rabbit pyr.actin. Pyrene fluorescence excited at 365 nm and monitored through a KV 389-nm filter, and 0.5 μM S1/0.55 μM *G368E* actin was displaced with 14 μM pyr.actin from rabbit. Conditions as Fig. 3 *b*.

ADP for acto-S1 can be defined by measuring the ADP inhibition of the ATP-induced dissociation of the complex (Siemankowski and White, 1984). This also showed no significant difference between the four actins, K_{ADP} (the dissociation constant of ADP for acto-S1) having a mean of 160 ± 20 μM for all of these actins.

Motility assays

The data presented in Figs. 6 and 7 were measured with the same batches of actin, polymerized and labeled at the same time. Fig. 6 shows the histograms of average filament velocity, moving on rabbit skeletal myosin, plotted with 1/3 μm s^{-1} bins for *Drosophila* wild-type, the two mutants, *E316K* and *G368E*, with RSA as a control. Apart from the *G368E* mutant, all of the actins gave a Gaussian distribution of velocity with rabbit (RSA) the fastest (mean, 2.51 μm s^{-1}) and wild-type and *E316K* slower at 1.60 and 1.35 μm s^{-1}, respectively. *G368E* was the slowest (1.29 μm s^{-1}) but with a clearly non-Gaussian distribution weighted to low velocities. The *Drosophila* actins produced a few high speed outliers between 4 and 6 μm s^{-1}, more than three standard deviations above the mean. When these experiments were repeated with HMM (30 μg/ml), all four actin filaments show (Fig. 7) Gaussian-like velocity profiles with RSA the fastest (5.20 μm s^{-1}) and *G368E* the slowest (3.30 μm s^{-1}). There were no differences in the mean velocities for wild-type and *E316K* at 3.93 μm s^{-1}, 24% slower than RSA. The quality of movement was, as reported by Homsher et al. (1992), better for HMM than for whole myosin substrates as there were fewer dead heads and rotating filaments, with the vast majority of filaments moving in fairly straight lines at more or less uniform velocities.

Separate control experiments were performed with entirely different batches of *Drosophila* actins, rabbit skeletal actin, and myosin. Actin from *KM88* flies was compared with wild-type, the mixed *KM88*/wild-type copolymer (formed by copolymerizing equimolar solutions of wild-type and *KM88*) and RSA moving on rabbit skeletal myosin. The velocities

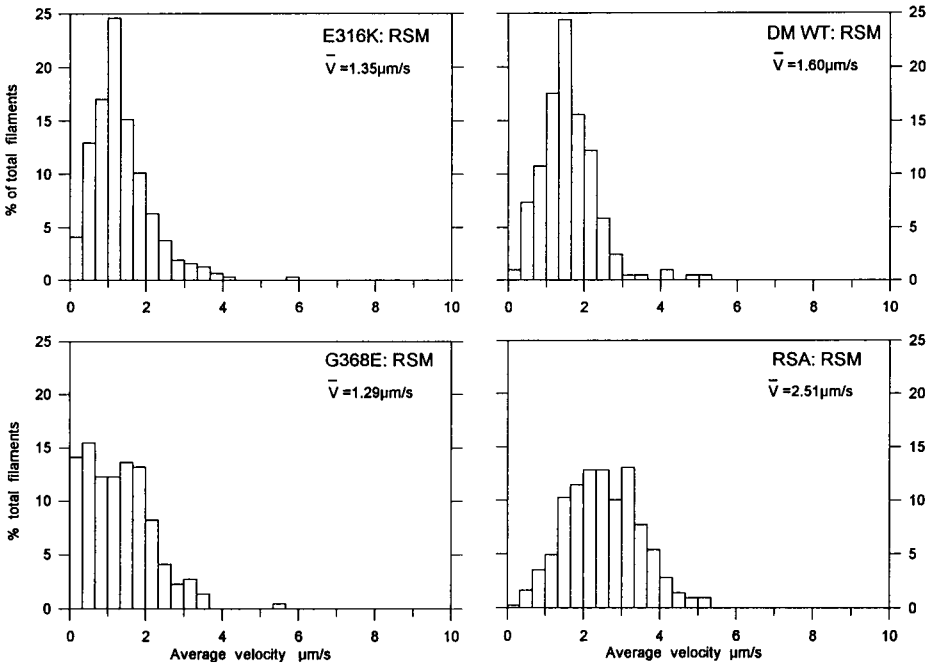

FIGURE 6 Motility in vitro of *Drosophila* and rabbit actins moving on rabbit myosin. Histograms are in 1/3 μm s^{-1} bins with average velocity V bar; full results are given in Table 2. The decrease in wild-type velocity compared with RSA is significant ($P < 10^{-15}$, Student's t-test). Similarly, both *E316K* and *G368E* are significantly slower than wild-type ($P < 10^{-3}$). The results for *E316K* and *G368E* are also significantly different ($P < 10^{-2}$, Kolmogrov test).

of wild-type (1.58 μm s^{-1}) and the mixed polymer (1.55 μm s^{-1}) were not significantly different. However, the velocity of *KM88* actin (1.77 μm s^{-1}) is slightly but significantly faster than wild-type, although still slower than RSA. The RSA controls were slower by 7% than those shown in Fig. 6 (2.33 μm s^{-1} and 2.51 μm s^{-1}, respectively). This may be partly accounted for by the difference in temperature, 0.2°C, between the two experiments and is within the estimated systematic errors between experiments of ±4%. No differences were seen between the wild-type, *KM88*, and the mixed polymer filaments moving on HMM; all were 22% slower than RSA.

The full results are presented in Table 2. Applying Student's t-test to the data shows that the velocity differences between myosin/RSA and myosin/*Drosophila* wild-type actin are highly significant. Indeed, all of the *Drosophila* actins move significantly slower than RSA on both myosin and HMM. The statistical moments of the myosin data show, in general, that the *Drosophila* actin filament velocity distributions are somewhat skewed to the low velocity side (positive third moment, skewness) and are more sharply peaked than a normal distribution (fourth moment, kurtosis greater than three); this does not apply to the RSA, which shows near-Gaussian statistics. In contrast, all of the data on HMM

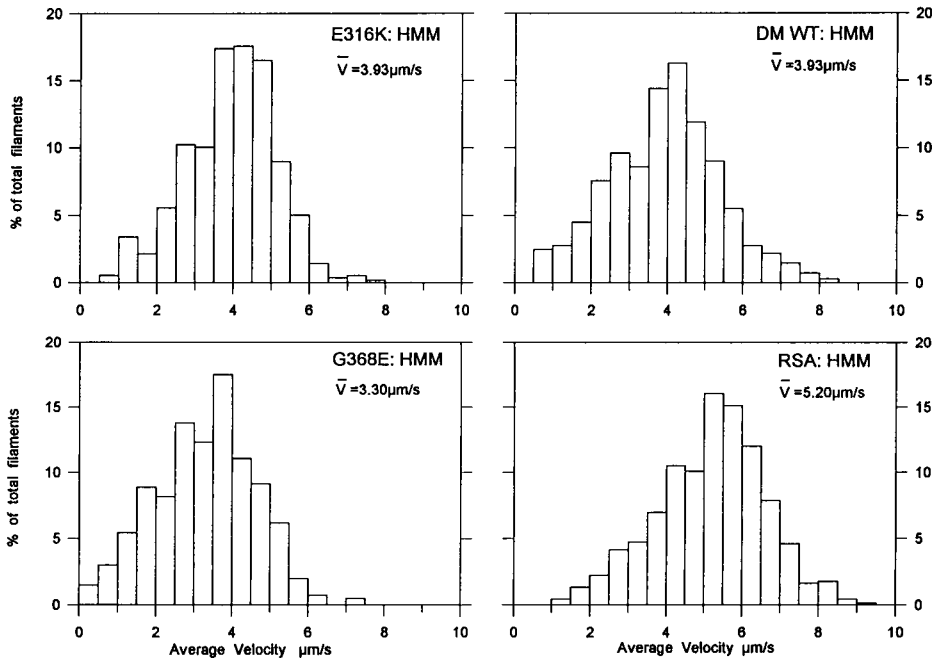

FIGURE 7 Motility in vitro of *Drosophila* and rabbit actins moving on rabbit HMM. Histograms are in 1/2 μm s^{-1} with average velocity V bar; full results are given in Table 2. The decrease in wild-type velocity compared with RSA is significant ($P < 10^{-14}$, Student's t-test), and *G368E* is significantly slower than wild-type or *E316K* ($P < 10^{-12}$.). Wild-type and *E316K* have the same velocity ($P > 0.9$). Temperature, 25°C.

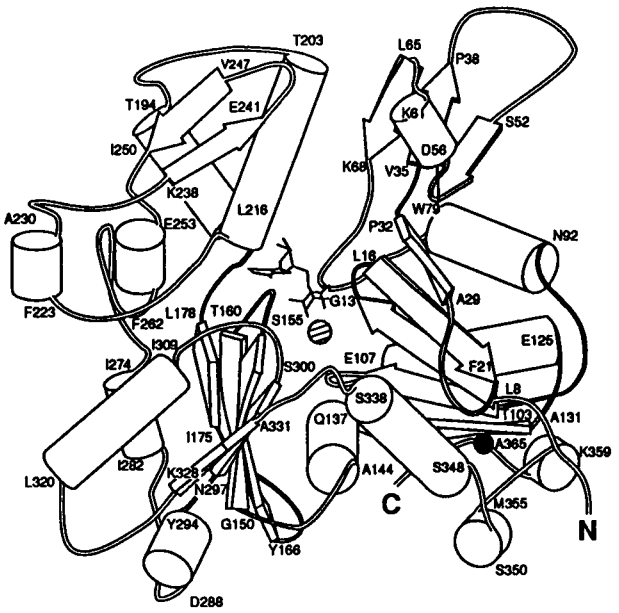

FIGURE 8 Actin structure, redrawn from Kabsch et al. (1990). The ATP molecule is shown, as are the positions of the divalent cation (hatched sphere) and residue 368 (filled sphere). E316 is in subdomain 3, forming part of the α-helix 309–320. Actin has been described as comprising four subdomains: subdomain 1, residues 1–32, 70–144, and 338–372; subdomain 2, residues 33–69; subdomain 3, residues 145–180 and 270–337; and subdomain 4, residues 181–269.

substrates are close to normal Gaussian distributions, indicating that the machine analysis is not responsible for abnormal statistics. Although the *KM88* filaments move significantly faster on myosin than *Drosophila* wild-type, the mixed polymers are not significantly different from wild-type in either experiment. The *G368E* actin moving on the myosin substrate produces a flat-topped velocity distribution that is clearly non-Gaussian. Therefore, skew and kurtosis are not strictly comparable. Student's *t*-test is inappropriate (Barlow, 1989) for determining significance when the means are close. Use of the Kolmogorov test shows that these results are significantly different ($P < 0.01$) from those of the other *Drosophila* actins.

DISCUSSION

The Drosophila actin preparations are >90% pure actin but consist of multiple actin isoforms, derived mostly from the *Act88F* and *Act79B* genes. Only in the case of the *E316K* actin preparations was it possible, because of the charge change, to separate all the actin isoforms on a two-dimensional gel. In these *E316K* preparations, the type I and II actins from the abdomen, legs, and head comprise 60% of the protein yield and have copurified with the *Act88F* actin through at least two cycles of depolymerization/polymerization. So, unless there are substantial differences in isoform polymerizability, the F-actins are likely to be copolymers of all the actin isoforms present. The level of non-*Act88F* actin isoforms, seen in *E316K* actin preparations and assumed to be present in the other preparations, limits the interpretations that can be made of the differences between the proteins analyzed here.

In this context it is important to distinguish between the two types of experiments undertaken, first, the steady-state ATPase and motility assays and, second, the transient kinetic measurements. In the first case, the measurements result from numerous repetitive interactions between myosin heads and several different actin molecules and thus reflect the average behavior of the actin population (steady-state assays) or the average behavior of the actins within a single filament (motility). For steady-state assays, it is a simple arithmetic average. In the transient experiments, the presence of two types of actin differing by more than a factor of three in the rate constant being assayed would give rise to biphasic exponentials. In no case were significant deviations from single exponentials observed and so this case does not apply. The presence of two types of actin differing by less than a factor of two would produce apparently single exponentials but with observed rates now intermediate between the two intrinsic values. For all parameters measured, the *Drosophila* actins behaved identically with one exception, the displacement reaction for S1 from *G368E*, which is discussed below. An assessment of how large a change in the property of an actin would have to be for it to be picked up in these measurements has to be dealt with on a case by case basis as it depends upon the signal-to-noise ratio as well as the relative sizes of the different actin populations. However, with the exception of the *G368E* displacement reaction, the results are consistent with all of the fly actins being identical to within a factor of two.

Comparison of *Drosophila* wild-type and *KM88* actins

The yields of actin from the *KM88* flies were lower than from the wild-type flies as might be expected as no IFM actin is expressed. We therefore performed a more limited series of measurements on the actin from these flies. Of the solution properties examined (Table 1), no significant differences were seen between the two actins. In the motility experiments, only on myosin was there a significant difference between wild-type and *KM88* velocities, the latter being 12% faster. The actin polymer prepared from a mixture of the wild-type and *KM88* preparations, which may be expected to contain only 20% pure wild-type *Act88F* isoform, was indistinguishable from actin prepared from wild-type flies. These results preclude the argument that the effects we find with mutant actins could be a result simply of a relative change in proportion of the *Act88F* actin and the contaminating isoforms, particularly in the case of the in vitro motility experiments in which the mutant actins show a decreased motility compared with wild-type, whereas the *KM88* actins show, if anything, an increased motility.

Thus, for the wild-type/mutant comparisons below, if a difference is seen in the two preparations, it must reflect a property of the (40%) mutant actin expressed. The true dif-

TABLE 2 Velocity measurements in vitro of *Drosophila* wild-type and mutant actin filaments moving on rabbit myosin and HMM

Myosin/actin	Number of filaments (n)	Average velocity (μm/s)	SE (μm/s)	SD (σ)	Skew (γ)	Kurtosis (κ)
HMM (25.2–25.4°C)						
G368E	405	3.301	0.065	1.31	−0.02	2.7
E316K	557	3.926	0.050	1.44	−0.09	3.2
DM WT	688	3.935	0.055	1.45	0.04	2.9
RSA	677	5.201	0.055	1.44	−0.09	3.2
Myosin (25.2–25.4°C)						
G368E	220	1.294	0.058	0.87	(0.94)	(0.48)
E316K	317	1.352	0.044	0.78	1.51	7.3
DM WT	205	1.599	0.051	0.73	1.46	7.6
RSA	428	2.506	0.046	0.95	0.21	2.7
Myosin (25°C)						
KM 88	1052	1.769	0.023	0.75	0.52	2.6
KM88/WT	1084	1.547	0.018	0.59	0.74	3.9
DM WT	463	1.580	0.028	0.60	0.68	3.5
RSA	841	2.327	0.030	0.86	0.35	2.7

For HMM, the decrease in wild-type velocity compared with RSA is significant ($P < 10^{-10}$, Student's *t*-test), and *G368E* is significantly slower than wild type or *E316K* ($P < 10^{-10}$). Wild-type and *E316K* have the same velocity ($P > 0.9$). For myosin, the decrease in wild-type velocity compared with RSA is significant ($P < 10^{-10}$, Student's *t*-test). Similarly, *E316K* and *G368E* are significantly slower than wild-type ($P < 10^{-3}$). The results for *E316K* and *G368E* are also significantly different ($P < 10^{-2}$, Kolmogorov test); wild-type and the KM88/WT mixed polymer are not significantly different ($P > 0.3$, Student's *t*-test) but KM88 is significantly different from wild-type ($P < 10^{-5}$), KM88/WT ($P < 10^{-10}$), and RSA ($P < 10^{-10}$).

ference between pure wild-type and pure mutant could be significantly greater. When no differences are seen between wild-type and mutant, then either the property observed is dominated by the nonflight muscle actins present or the actin mutation has not changed the property observed.

Comparison of rabbit and *Drosophila* wild-type actins

Actin is one of the most highly conserved proteins known. The mature *Drosophila Act88F* wild-type actin has only 28 amino acid sequence differences of a total of 374 residues, from rabbit skeletal α-actin (see Hennessey et al., 1993; Sheterline and Sparrow, 1994, for reviews). The *Drosophila* actin has 1 less acidic amino acid and 5 substitutions in the first 10 NH_2-terminal residues, which form part of subdomain 1 (residues 1–32, 70–144, and 338–372; see Fig. 8) and 7 further changes in this subdomain. There are 10 and 6 substitutions in subdomain 3 (residues 145–180 and 270–337) and subdomain 4 (residues 181–269), respectively. Many of the substitutions are conservative. Few of these substitutions in the *Drosophila Act88F* actin are in proposed binding sites. The exception is the extreme NH_2 terminus where loss of an acidic residue and 2 conservative substitutions (glutamate to aspartate) occur in a cluster of negative charges (amino acids 1–4) predicted to form electrostatic interactions with the myosin head (Rayment et al., 1993a; Schroeder et al., 1993). These sequence differences may explain the different kinetics of rabbit skeletal actin and *Drosophila* wild-type. However, although the D1H and D4H mutations in *Dictyostelium* actin (Sutoh et al., 1991) decreased the V_{max} for actin-activated ATPase activity and in vitro motility, K_{app} was not affected, implying that the negative charges at the NH_2 terminus may not be so important in determining this parameter as our comparison of rabbit and *Drosophila* wild-type might suggest.

The steady-state rabbit S1-Mg-ATPase activations by *Drosophila* wild-type and rabbit actins show no differences in the maximal ATPase rate achieved at low ionic strengths. However, there is an increase in K_{app} for wild-type compared with rabbit actin and decreased in vitro velocities of the *Drosophila* actin on both rabbit myosin and HMM (64 and 75%, respectively). A doubling in velocity for rabbit actin moving on HMM compared with myosin is consistent with previous reports (Higashi-Fujime, 1991 and Homsher et al., 1992). In view of the sequence differences, it may not be surprising that the velocity of *Drosophila* actin is different from that of rabbit actin when moving on rabbit myosin or HMM. The close similarity in the velocities obtained in motility assays done many months apart with completely different preparations of myosin, RSA, and wild-type *Drosophila* actins (Table 2) gives an indication of the reliability of these measurements.

Kron and Spudich (1986) reported a small but, in their experiment not significant, reduction (9%) in the in vitro velocity of actin from the slime mold, *Dictyostelium discoideum*, compared with RSA when moving on rabbit myosin. Although the in vitro motilities on HMM with *Dictyostelium* actin were significantly lower (Sutoh et al. 1991; Johara et al., 1993) than the results for rabbit and *Drosophila* wild-type presented here, the V_{max} for actin-activated myosin Mg-ATPase that they obtained with *Dictyostelium* actin was significantly higher. However, they did not measure the velocity of RSA filaments. Aspenström et al. (1992a, b) and Cook et al. (1993) saw reductions in the rabbit S1-ATPase activated by β-actin and yeast (*Saccharomyces cerevisiae*) wild-type actin compared with RSA, but neither group saw significant reductions in in vitro velocities on rabbit myosin. However, Kron et al. (1992) reported a 50% reduction in the in vitro velocity of yeast wild-type actin compared with RSA moving on rabbit S1. Some correlation between in vitro motility and

the V_{max} for actin-activated myosin Mg-ATPase activity seems to be generally accepted, but data from a number of sources show that this is, at best, only a trend (see discussion in Homsher et al., 1992). It is difficult to make clear conclusions on the relationship between the reduced motility but unchanged V_{max} of *Drosophila* actin compared with rabbit, especially when the velocity reduction is so small.

The differences in the interaction of *Drosophila* and rabbit α-actin with rabbit myosin and its fragments in the steady state were also apparent for the affinity of actin for nucleotide-free S1, estimated from the ratio k_{off}/k_{on}. This was due to a reduction in k_{on}, as no difference was apparent in the rate of displacement of two actins from acto-S1 (k_{off}).

The reduced affinity of wild-type actin for S1 as seen in both k_{on} and K_{app} could result from the loss of one negative charge in the NH_2 terminus of the wild-type actin compared with rabbit. This is a region thought to be involved in an electrostatic interaction with S1, and the marked ionic strength dependence of k_{on} suggests a strong electrostatic component involved in this initial binding (White and Taylor, 1976; Geeves and Goldman, 1990). All other kinetic measurements showed no significant difference between the rabbit and wild-type actins. It will be of interest to know whether this reduced interaction of the wild-type actin with rabbit S1 reflects an intrinsic property of the wild-type actin or simply reflects the divergence in the complementary actin/myosin binding sites of the native partner proteins.

E316K

In all of the measurements reported here no significant differences were found between the wild-type and *E316K* actins except for the velocity of movement on a rabbit myosin substrate. This replacement of a glutamate by lysine in subdomain 3 (Fig. 8) is remote from the myosin binding site and therefore expected to have no direct influence on the interaction with myosin. It is not clear why the *E316K* actin should show a decreased in vitro velocity on myosin, especially when it does not do so on HMM. These myosin molecules differ only in that HMM lacks the light meromyosin α-helical coiled-coil region. Residue E316 is close to the proposed tropomyosin binding site (Holmes, personal communication), which may explain the effects of the *E316K* mutation on fiber mechanics (Drummond et al., 1990). Experiments are in progress to reconstitute thin filaments containing *E316K* actin with rabbit tropomyosin and troponin to seek any effects of this mutation on regulation. However, *E316K* increases profilin binding (Drummond et al., 1991a), although it does not lie within the profilin binding site, which includes subdomain 1 (Schutt et al., 1993), and this may indicate that this mutation has slight, but long range conformational effects.

G368E

G368E filaments show a reduction in velocity when moving on either rabbit myosin (19%) or HMM (16%) compared with wild-type actin. As with the two other *Drosophila* actins (wild-type and *E316K*), *G368E* actin produces velocity distributions that are different from that of rabbit actin, which is truly Gaussian with Normal statistics. Whereas the *Drosophila* wild-type and *E316K* data have near-Normal distributions with some skew and sharp peaks, *G368E* is clearly not Normal. The presence of mixed isoforms in the *Drosophila* actin preparations may explain these results, with the *G368E* mutation additionally increasing the magnitude of the effects. This proposal can be tested only by purifying the separate isoforms.

In the steady-state ATPase assay for *G368E*, the V_{max} and K_{app} are very similar to wild-type. The rate of *G368E* actin binding to S1 also shows a small decrease but at the limits of experimental accuracy. However, significant differences were seen in the k_{off}, which is more than twofold larger than for wild-type (or *E316K*). The ratio k_{off}/k_{on} (K_d) thus shows a threefold increase, and an increase in K_d was also detected in the titration experiment.

In comparison with wild-type *Drosophila* actin, the reductions the *G368E* actin shows in its affinity for rabbit myosin in solution and in its in vitro motility are similar to those found in vivo for wingbeat frequency and the delayed tension rate constant (Drummond et al., 1990). It is difficult to make direct comparisons between individual rate constants and a macroscopic property like the rates of tension transients and velocity in motility measurements, as many processes probably contribute to these macroscopic events. However, the following points are worth making. Myosin binds to actin in at least two ways, an initial relatively weak binding followed by an isomerization to a strongly binding, force-holding state.

$$\mathrm{A + M.N} \overset{K_1}{\leftrightarrow} \underset{\text{A-state}}{\mathrm{A\text{-}M.N}} \overset{K_2}{\leftrightarrow} \underset{\text{R-state}}{\mathrm{A.M.N}} \qquad (1)$$

The isomerization is coupled to events at the myosin active site. One interpretation of these events is that these two binding steps occur for S1 whatever nucleotide is bound in the active site, but the extent of the isomerization (the equilibrium constant) depends upon the nucleotide bound (see Geeves, 1991). For this model, an increase in k_{off} can caused by an increase in k_{-1} (weaker binding to the A-state), a decrease in K_2 (weaker isomerization to the R-state), or a combination of the two. Thus, a change in *G368E* could affect the ability of actin to bind into the weakly binding pre-force-generating A-state or its ability to isomerize. The P_i concentration dependence of both P_i and pressure-induced tension transients in skinned rabbit muscle fibers have been interpreted as being the result of an isomerization between a weakly binding A-M.ADP.P_i state and a strongly binding force-holding A.M.ADP:P_i state, equivalent to step 2 above (Fortune et al., 1991; Homsher and Millar, 1990; Dantzig et al., 1992). Thus, an effect of the *G368E* mutation on this isomerization process could be compatible with both the reduced rate of delayed tension rise in mechanical

measurements and a reduction in K_2 in solution studies. No such simple correlation can yet be made for velocity measurements.

The myosin binding sites on actin lie on the front of the molecule in the standard view (Fig. 8) largely on subdomain 1 (Rayment et al., 1993a; Schroeder et al., 1993). Residue 368 lies on the rear surface of subdomain 1, with the side chain sticking out of the molecule (Fig. 9). Quanta molecular graphics software (Molecular Simulations, Cambridge, UK) was used to substitute the glutamate into position 368 (Fig. 9) of the atomic structure of rabbit skeletal actin determined by Kabsch et al. (1990). This showed that such a change in residue needs no alterations in the positions of neighboring atoms as, in three of eight standard glutamate conformations investigated, no close atomic contacts occur. Bearing in mind that this is done in a static model and that this side chain sticks out into solution, this would imply that the effects of the *G368E* mutation are more likely to affect a ligand binding site than cause a conformational change. The obvious ligand binding to be affected must be the myosin. It seems unlikely that a direct contact between this residue and the myosin heavy chain could be made (see Rayment et al., 1993a; Schroeder et al., 1993). However, reconstructions of electron micrographs of F-actin decorated with S1 show that S1A1 makes an additional contact compared with S1A2 in this region of actin (Milligan et al., 1990). The only difference between these S1 species is that S1A1 contains the LC1 alkaline light chain, which contains a 41-residue NH_2-terminal extension compared with the LC3 of S1A2. It thus appears likely that this extension of LC1 makes a contact with the COOH terminus of actin. Additional support for this comes from cross-linking studies (Sutoh, 1982) and nuclear magnetic resonance (Trayer et al., 1987). Although this interaction may explain the differences in wild-type and *G368E* actin described in this report, it leaves unresolved the explanation of what happens in *Drosophila* fibers as the alkaline light chain of *Drosophila* has no such NH_2-terminal extension (Falkenthal et al., 1984). The *G368E* mutation causes a small reduction (25%) in the binding of the actin to ATP (Drummond et al., 1992). Because *G368* is not close to the ATP binding site (Kabsch et al., 1990) and the mutant protein does not exhibit abnormal mobility in nondenaturing gels (Drummond et al., 1991b), this evidence might imply that the mutation has small conformational effects on subdomain 1.

Mutations in residues within the proposed myosin binding site have been made. Mutations of the NH_2-terminal acidic residues 1–4 (Sutoh et al., 1991; Aspenström and Karlsson, 1991; Aspenström et al., 1992b) can abolish S1 binding (*D3K.D4K*) or reduce in vitro motility (D1H, D1H.D4H, *D3Δ*.D4Δ, *D3A.D4A*). Similarly, the *D24.D25* mutation leads to a loss of sliding ability and actin activation of myosin ATPase but not rigor binding, and *E99H.E100H* leads to a partial loss of motility (Johara et al., 1993).

However, mutations in other residues that are not implicated in myosin binding have also been shown to have effects on actomyosin interactions. The *G245D* and *G245K* mutations have effects on actomyosin interactions (Aspenström et al., 1992a) as do the *P38A* and *C374S* mutations (Aspenström et al., 1993), although in these four cases there are also major effects on mutant actin polymerizability, suggesting that actin-actin interactions within F-actin filaments may affect in vitro motility. Residues 368 and 316 are not implicated in actin-actin binding in the F-actin model of Holmes et al. (1990). However, effects on F-actin structure may explain the effects of the *E316K* mutation, although how this might occur is not clear from the F-actin models.

Our purpose in performing the experiments reported here has been to study the in vitro properties of the *G368E* and *E316K* mutant actins. Such studies are necessary if we are to understand the effects of actin mutations on actomyosin function as a means to understanding the molecular details of the cross-bridge cycle. The advantage of studying mutants of the *Drosophila Act88F* gene is that we were able to show in vivo effects on flight ability and wingbeat frequency (*G368E*) together with changed rate constants for delayed tension development in demembranated fibers (*G368E* & *E316K*) and fiber stiffness (*G368E*) (Drummond et al., 1990) as well as studying the effects of the same mutations in vitro. Our goal is to use mutations to detect changes that occur in actin and myosin during the cross-bridge cycle and how these relate to the generation of tension. Our current inability to explain the effects of these mutations from the in vivo and in vitro measurements, especially in the case of *E316K*, which is remote from the proposed myosin binding site and must therefore have allosteric effects on actomyosin interactions, only serves to highlight the gulf between our knowledge of the actin and S1 structures and an understanding of the dynamic aspects of how these molecules interact.

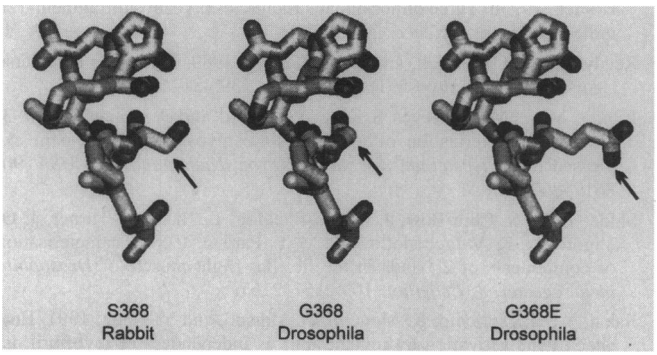

FIGURE 9 Actin structure: licorice model of amino acids 364–372 produced by using Quanta graphics (Molecular Simulations) from atomic coordinates of the structure described in Kabsch et al. (1990). From left to right are the structures of rabbit α-actin (S368) and versions in which mutations were made within the rabbit structure to alter residue 368 to produce the *Drosophila* wild-type (G368) and the *G368E* mutation. This structure lies on the surface of subdomain 1 with the solvent to the right.

M. A. wishes to thank Dr. Shahid Khan (Einstein College of Medicine, Yeshiva University, New York, NY) in whose laboratory the analysis of the filament motility data was done and Prof. H. Faulstich (Max Planck Institue for Medical Research, Heidelberg, Germany) for the gift of rhodamine-labeled phalloidin. We thank Drs. David White, Justin Molloy, and Jane Reed for helpful discussions and Birgit Brandmeyer and Anne Lawn for excellent technical support. For Fig. 9 we thank Prof. Guy Dodson and Dr.

Rod Hubbard for their help and our use of their molecular graphics facilities within the Department of Chemistry, University of York.

We acknowledge support from the Wellcome Trust (M.D.R. and M.A.G.), the Royal Society (M.A.G.), and Science and Engineering Research Council (E.S.H., D.R.D., and J.C.S.).

REFERENCES

Anson, M. 1992. Temperature dependence and Arrhenius activation energy of F-actin velocity generated in vitro by skeletal myosin. *J. Mol. Biol.* 224:1029–1038.

Aspenström, P., H. Engkvist, U. Lindberg, and R. Karlsson. 1992a. Characterization of yeast-expressed β-actins, site-specifically mutated at the tumor-related residue Gly245. *Eur. J. Biochem.* 207:315–320.

Aspenström, P., and R. Karlsson. 1991. Interference with myosin subfragment-1 binding by site-directed mutagenesis of actin. *Eur. J. Biochem.* 200:35–41.

Aspenström, P., U. Lindberg, and R. Karlsson. 1992b. Site-specific amino-terminal mutants of yeast-expressed β-actin. *FEBS Lett.* 303:59–63.

Ball, E., C. C. Karlik, C. J. Beall, D. L. Saville, J. C. Sparrow, and E. A. Fyrberg. 1987. Arthrin, a myofibrillar protein of insect flight muscle, is an actin-ubiquitin conjugate. *Cell.* 51:221–228.

Barlow, R. J. 1989. Statistics: A Guide to the Use of Statistical Methods in the Physical Sciences. John Wiley and Sons, Chichester, UK.

Bullard, B., R. Dabrowska, and L. Winkelman. 1973. The contractile and regulatory proteins of insect flight muscle. *J. Biochem.* 135:277–286.

Cook, R. K., D. Root, C. Miller, E. Reisler, and P. A. Rubenstein. 1993. Enhanced stimulation of myosin subfragment 1 ATPase activity by addition of negatively charged residues to the yeast actin NH_2 terminus. *J. Biol. Chem.* 268:2410- 2415.

Criddle, A. H., M. A. Geeves, and T. Jeffries. 1985. The use of actin labelled with *N*-(1-pyrenyl) iodoacetamide to study the interaction of actin with myosin subfragments and troponin/tropomyosin. *Biochem. J.* 232: 343–349.

Dantzig, J. A., Y. E. Goldman, N. C. Millar, J. Lactis, and E. Homsher. 1992. Reversal of the crossbridge force generating transition by photogeneration of phosphate in rabbit psoas muscle fibers. *J. Physiol.* 451:247–278.

Drummond, D. R., E. S. Hennessey, and J. C. Sparrow. 1991a. Characterisation of missense mutations in the *Act88F* gene of *Drosophila melanogaster*. *Mol. Gen. Genet.* 226:70–80.

Drummond, D. R., E. S. Hennessey, and J. C. Sparrow. 1991b. Stability of mutant actins. *Biochem. J.* 374:301–303.

Drummond, D. R., M. Peckham, J. C. Sparrow, and D. C. S. White. 1990. Alterations in crossbridge kinetics caused by mutations in actin. *Nature.* 348:440–442.

Falkenthal, S., V. P. Parker, W. W. Mattox, and N. Davidson. 1984. *Drosophila melanogaster* has only one myosin alklai light-chain gene which encodes a protein with considerable amino acid homology to chicken myosin alkali light chains. *Mol. Cell. Biol.* 4:956–965.

Faulstich, H., S. Zobeley, G. Rinnerthaler, and J. V. Small. 1988. Fluorescent phallotoxins as probes for filamentous actin. *J. Muscle Res. Cell Motility.* 9:370–383.

Fortune, N. S., M. A. Geeves, and K. W. Ranatunga. 1991. Tension responses to rapid pressure perturbations in glycerinated rabbit muscle fibers. *Proc. Natl. Acad. Sci. USA.* 88:7323–7327.

Fyrberg, E. A., J. W. Mahaffey, B. J. Bond, and N. Davidson. 1983. Transcripts of the six *Drosophila* actin genes accumulate in a stage- and tissue-specific manner. *Cell.* 33:115–123.

Geeves, M. A. 1991. The dynamics of actin and myosin association and the crossbridge model of muscle contraction. *Biochem. J.* 274:1–14.

Geeves M. A, and W. H. Goldman. 1990. Influence of anions, ionic strength and organic solvents on the interaction between actin and myosin S1. *Biochem. Soc. Trans.* 18:584–585.

Hennessey, E. S., D. R. Drummond, and J. C. Sparrow. 1993. Molecular genetics of actin function. *Biochem. J.* 291:657–671.

Higashi-Fujime, S. 1991. Reconstitution of active movement in vitro based on the actomyosin interaction. *Int. Rev. Cytology.* 125:95–138.

Hiratsuka, T. 1983. New ribose-modified fluorescent analogs of adenine and guanine nucleotides available as substrates for various enzymes. *Biochim. Biophys. Acta.* 742:496–508.

Hiromi, Y., and Y. Hotta. 1985. Actin gene mutations in *Drosophila*: heat-shock activation in the indirect flight muscles. *EMBO J.* 4:1681–1687.

Hiromi, Y., H. Okamoto, W. J. Gehring, and Y. Hotta. 1986. Germline transformation with *Drosophila* mutant actin genes induces constitutive expression of heat shock genes. *Cell.* 44:293–301.

Holmes, K. C., D. Popp, W. Gebhard, and W. Kabsch. 1990. Atomic model of the actin filament. *Nature.* 347:44–49.

Homsher, E., and N. C. Millar. 1990. Caged compounds and striated muscle contraction. *Annu. Rev. Physiol.* 52:875–896.

Homsher, E., F. Wang, and J. R. Sellers. 1992. Factors affecting movement of F-actin filaments propelled by skeletal muscle heavy meromyosin. *Am. J. Physiol.* 262:C714-C723.

Horovitch, S. J., R. V. Storti, A. Rich, and M. L. Pardue. 1979. Multiple actins in *Drosophila melanogaster*. *J. Cell Biol.* 82:86–92.

Johara, M., Y. Y. Toyoshima, A. Ishijima, H. Kojima, T. Yanagida, and K. Sutoh. 1993. Charge-reversion mutagenesis of *Dictyostelium* actin to map the surface recognized by myosin during ATP-driven sliding motion. *Proc. Natl. Acad. Sci. USA.* 90:2127–2131.

Kabsch, W., H. G. Mannherz, D. Suck, E. F. Pai, and K. C. Holmes. 1990. Atomic structure of the actin: DNase I complex. *Nature.* 347:37–44.

Kron, S. J., D. G. Drubin, D. Botstein, and J. A. Spudich. 1992. Yeast actin filaments display ATP-dependent sliding movement over surfaces coated with rabbit muscle myosin. *Proc. Natl. Acad. Sci. USA.* 89:4466–4470.

Kron, S. J., and J. A. Spudich. 1986. Fluorescent actin filaments move on myosin fixed to a glass surface. *Proc. Natl. Acad. Sci. USA.* 83:6272–6276.

Kron, S. J., Y. Y. Toyoshima, T. Q. P. Uyeda, and J. A. Spudich. 1991. Assays for actin sliding movement over myosin-coated surfaces. *Methods Enzymol.* 196:399–416.

Lehrer, S. S., and G. Kerwar. 1972. Intrinsic fluorescence of actin. *Biochemistry.* 11:1211–1217.

Mahaffey, J. W., M. D. Coutu, E. A. Fyrberg, and W. Inwood. 1985. The flightless *Drosophila* mutant *raised* has two distinct genetic lesions affecting accumulation of myofibrillar proteins in flight muscles. *Cell.* 40: 101–110.

Margossian, S. S., and S. Lowey. 1982. Preparation of myosin and its subfragments from rabbit skeletal muscle. *Methods Enzymol.* 85:55–71.

Milligan, R. A., M. Whittaker, and D. Safer. 1990. Molecular structure of F-actin and location of surface binding sites. *Nature.* 348:217–221.

Mogami, K., and Y. Hotta. 1981. Isolation of *Drosophila* flightless mutants which affect myofibrillar proteins of insect flight muscle. *Mol. Gen. Genet.* 183:409–417.

Pardee, J. D., and J. A. Spudich. 1982. Purification of muscle actin. *Methods Cell Biol.* 24:271–289.

Rayment, I., H. M. Holden, M. Whittaker, C. B. Yohn, M. Lorenz, K. C. Holmes, and R. A. Milligan. 1993a. Structure of the actin-myosin complex and its implications for muscle contraction. *Science.* 261:58–65.

Rayment, I., W. R. Rypniewski, K. Schmidt-Bäse, R. Smith, D. R. Tomchick, M. M. Benning, D. A. Winkleman, G. Wesenber, and H. M. Holden. 1993b. Three dimensional structure of myosin subfragment-1: a molecular motor. *Science.* 261:50–58.

Reedy, M. C., C. J. Beall, and E. A. Fyrberg. 1989. Formation of reverse rigor chevrons by myosin heads. *Nature.* 339:481–483.

Ritchie, M. D., M. A. Geeves, S. K. A. Woodward, and D. J. Manstein. 1993. Kinetic characterization of a cytoplasmic myosin motor domain expressed in *Dictyostelium discoideum*. *Proc. Natl. Acad. Sci. USA.* 90: 8619–8623.

Saide, J. D., S. Chin-Bow, J. Hogan-Sheldon, L. Busquets-Turner, J. O. Vigoreaux, K. Valgeirsdottir, and M. L. Pardue. 1989. Characterisation of components of Z bands in the fibrillar flight muscle of *Drosophila melanogaster*. *J. Cell Biol.* 109:2157–2167.

Sakai, Y., H. Okamoto, K. Mogami, H. Matsuo, and Y. Hotta. 1991. Heat shock gene activation by mutant actin is independent of myofibril degeneration in *Drosophila* muscle. *J. Biochem.* 109:670–673.

Sakai, Y., H. Okamoto, K. Mogami, T. Yamada, and Y. Hotta. 1990. Actin with tumor-related mutation is antimorphic in *Drosophila* muscle: two distinct modes of myofibrillar disruption by antimorphic actins. *J. Biochem.* 107:499–505.

Schroeder, R. R., D. J. Manstein, W. Jahn, H. Holden, I. Rayment, K. C. Holmes, and J. A. Spudich. 1993. Three-dimensional atomic model of F-actin decorated with *Dictyostelium* myosin. *Nature.* 364:171–174.

Schutt, C. E., J. C. Myslik, M. D. Rozycki, N. C. W. Goonesekere, and U. Lindberg. 1993. The structure of crystalline profilin: β-actin. *Nature.* 365:810–816.

Sellers, J. R., G. Cuda, F. Wang, and E. Homsher. 1993. Myosin-specific adaptations of the motility assay. *In* Methods in Cell Biology, Vol. 39: Motility Assays for Motor Proteins. J. M. Scholey, editor. Academic Press, London. 23–49.

Sheterline, P., and J. C. Sparrow. 1994. 'Actin' in Protein Profiles. P. Sheterline, series editor. Academic Press, London.

Siemankowski, R. F., and H. D. White. 1984. Kinetics of the interaction between actin, ADP and cardiac myosin-S1. *J. Biol. Chem.* 259:5045–5053.

Sparrow, J., M. Reedy, E. Ball, V. Kyrtatas, J. Molloy, J. Durston, E. Hennessey, and D. White. 1991. Functional and ultrastructural effects of a missense mutation in the indirect flight muscle-specific actin gene of *Drosophila melanogaster. J. Mol. Biol.* 222:963–982.

Sutoh, K. 1982. Identification of myosin-binding sites on the actin sequence. *Biochemistry.* 21:3654–3661.

Sutoh, K., M. Ando, K. Sutoh, and Y. Y. Toyoshima. 1991. Site-directed mutations of *Dictyostelium* actin: disruption of a negative charge cluster at the N terminus. *Proc. Natl. Acad. Sci. USA.* 88:7711–7714.

Szilagyi, L., and R. Chen Lu. 1982. Changes of lysine reactivities of actin in complex with myosin subfragment-1, tropomyosin and troponin. *Biochem. Biophys. Acta.* 709:204–211

Trayer, I. P, H. R. Trayer, and B. A. Levine. 1987. Evidence that the N-terminal region of A1-light chain of myosin interacts directly with the C-terminal region of actin: a proton magnetic resonance study. *Eur. J. Biochem.* 164:259–266.

Warrick, H. M., R. M. Simmons, J. T. Finer, T. Q. P. Uyeda, S. Chu, and J. A. Spudich. 1993. In vitro methods for measuring force and velocity of the actin-myosin interaction using purified proteins. *In* Methods in Cell Biology, Vol. 39: Motility Assays for Motor Proteins. J. M. Scholey, editor. Academic Press, London. 1–21.

Weeds, A. G., and R. S. Taylor. 1975. Separation of subfragment-1 isoenzymes from rabbit skeletal muscle myosin. *Nature.* 257:54–56.

White, D. C. S. 1983. The elasticity of relaxed insect fibrillar flight muscle. *J. Physiol.* 343:31–57.

White, H. D., and E. Taylor 1976. The energetics and mechanism of actomyosin ATPase. *Biochemistry.* 15:5818–5826.

Woodward, S. K. A., J. F. Eccleston, and M. A. Geeves. 1991. Kinetics of the interaction of 2′(3′)-*O*-(*N*-methylanthraniloyl)-ATP with myosin subfragment 1 and actomyosin subfragment 1: characterisation of two acto. S1. ADP complexes. *Biochemistry.* 30:422–430.